Thermodynamics of Electron Transfer in Oxygenic Photosynthetic Reaction Centers: Volume Change, Enthalpy, and Entropy of Electron-Transfer Reactions in Manganese-Depleted Photosystem II Core Complexes†

Jian-Min Hou,‡ Vladimir A. Boichenko,‡,§ Bruce A. Diner,|| and David Mauzerall*,‡

The Rockefeller University, 1230 York Avenue, New York, New York 10021, Institute of Basic Biological Problems, Russian Academy of Sciences, Pushchino 142290, Russia, and Experimental Station, Central Research and Development Department, E. I. du Pont de Nemours & Company, Wilmington, Delaware 19880-0173

Received August 31, 2000; Revised Manuscript Received April 19, 2001

ABSTRACT: We have previously reported the thermodynamic data of electron transfer in photosystem I using pulsed time-resolved photoacoustics [Hou et al. (2001) *Biochemistry 40*, 7109−7116]. In the present work, using preparations of purified manganese-depleted photosystem II (PS II) core complexes from *Synechocystis* sp. PCC 6803, we have measured the ΔV, ΔH, and estimated $T\Delta S$ of electron transfer on the time scale of 1 μs. At pH 6.0, the volume contraction of PS II was determined to be -9 ± 1 Å^3. The thermal efficiency was found to be $52 \pm 5\%$, which corresponds to an enthalpy change of -0.9 ± 0.1 eV for the formation of the state $P_{680}^+Q_A^-$ from P_{680}*. An unexpected volume expansion on pulse saturation of PS II was observed, which is reversible in the dark. At pH 9.0, the volume contraction, the thermal efficiency, and the enthalpy change were -3.4 ± 0.5 Å^3, $37 \pm 7\%$, and -1.15 ± 0.13 eV, respectively. The ΔV of PS II, smaller than that of PS I and bacterial centers, is assigned to electrostriction and analyzed using the Drude−Nernst equation. To explain the small ΔV for the formation of $P_{680}^+Q_A^-$ or $Y_Z^{\bullet}Q_A^-$, we propose that fast proton transfer into a polar region is involved in this reaction. Taking the free energy of charge separation of PS II as the difference between the energy of the excited-state P_{680}* and the difference in the redox potentials of the donor and acceptor, the apparent entropy change ($T\Delta S$) for charge separation of PS II is calculated to be negative, -0.1 ± 0.1 eV at pH 6.0 ($P_{680}^+Q_A^-$) and -0.2 ± 0.15 eV at pH 9.0 ($Y_Z^{\bullet}Q_A^-$). The thermodynamic properties of electron transfer in PS II core reaction centers thus differ considerably from those of bacterial and PS I reaction centers, which have ΔV of ~ -27 Å^3, ΔH of ~ -0.4 eV, and $T\Delta S$ of $\sim +0.4$ eV.

Oxygenic photosynthesis in cyanobacteria, algae, and higher plants involves the cooperation of two photosystems (PS),[1] PS I and PS II (*1*). PS II is an integral membrane protein complex of more than 19 subunits and carries out the initial step of oxygenic photosynthesis. It utilizes light energy to generate oxidized primary electron donor P_{680}^+ and reduced quinone electron acceptor Q_A^-. P_{680}^+ oxidizes tyrosine Y_Z, which in turn oxidizes the Mn cluster, the site of water oxidation to oxygen.

The first three-dimensional structure of a water-oxidizing PS II complex from *Synechococcus elongatus* at 3.8 Å resolution provides direct information of detailed orientation and interaction of cofactors and protein subunits (*2*). It shows that the heart of PS II consists of the D1 and D2 proteins, which bind P_{680} (primary electron donor), pheophytin (primary acceptor), and Q_A and Q_B (quinone secondary acceptors). Y_Z, the tyrosine electron donor to P_{680}^+, is located at the D1-161 position.

The kinetics of the electron-transfer steps in photosynthetic reaction centers has been thoroughly investigated over the complete time scale of femtoseconds to many seconds (*3*, *4*). The early processes occurring in PS II revealed by ultrafast spectroscopy can be divided into several steps: (a) absorption of light quanta by antenna to form excited states of pigments; (b) trapping of excitation energy by the primary electron donor P_{680} in the reaction center on the picosecond time scale; (c) primary charge separation from the singlet excited state of P_{680} to the primary acceptor Pheo in about 3−20 ps; (d) stabilization of the separated charges from the radical pair $P_{680}^+Pheo^-$ on the acceptor side by electron transfer to Q_A in about 200 ps and to Q_B on the hundreds-of-microseconds time scale; and (e) on the donor side, an electron is supplied to reduce P_{680}^+ from a tyrosine residue (Y_Z) on the nanosecond to microsecond time scale. It has been reported that the electron transfer from Y_Z to P_{680}^+ is dependent on the ambient pH of the PS II preparations (*5*,

† This work is supported by grants from the NSF (MCB 99-04522) and NIH (GM 25693) to D.M. and from NRICGP/USDA (97-35306-4882) to B.A.D.

* Corresponding author. E-mail: mauzera@rockvax.rockefeller.edu. Fax: (212) 327-8853.

‡ The Rockefeller University.

§ Russian Academy of Sciences.

|| E. I. du Pont de Nemours & Co.

[1] Abbreviations: Ches, 2-(*N*-cyclohexylamino)ethanesulfonic acid; DM, dodecyl β-D-maltoside; FeCy, potassium ferricyanide; Hepes, *N*-(2-hydroxyethyl)piperazine-*N*′-2-ethanesulfonic acid; Mes, 2-(*N*-morpholino)ethanesulfonic acid; Mops, 3-(*N*-morpholino)propanesulfonic acid; PA, photoacoustic(s); PS, photosystem; PTRPA, pulsed time-resolved photoacoustics; TE, thermal efficiency.

10.1021/bi010373s CCC: $20.00
Published on Web 05/22/2001

6). The rate of electron transfer of this step is between tens to hundreds of nanoseconds in intact PS II at physiological pH and hundreds of nanoseconds in apo-PS II at pH 9. However, at acidic pH this rate in apo-PS II is slowed about 10−100-fold, i.e., to >10 μs. There are no studies on the thermodynamic properties of these intermediates.

Photoacoustic (PA) measurements have proven to be a useful tool for the study of the thermodynamics of electron transfer in chemical and biological systems (*7*−*9*). Although it is the free energy which determines the equilibrium of a chemical reaction, decomposition of this energy into terms of enthalpy and entropy allows an initial separation of the driving forces of the reaction: bonding or interaction energies and entropic or available states of the system. This decomposition is particularly important for reactions involving proteins where entropic changes can be large and can characterize the often hypothesized but rarely observed changes in conformation.

By use of pulsed time-resolved photoacoustics (PTRPA) one can measure directly the volume change (ΔV), the enthalpy (ΔH), and, via the free energy (ΔG), the entropy ($T\Delta S$) in electron-transfer reactions (*8*). We have previously measured these parameters in the photosynthetic reaction center complexes from *Rhodobacter sphaeroides* (*9*). In the preceding paper (*10*), our study of the thermodynamics of electron transfer in the PS I trimer complex from *Synechocystis* PCC 6803 similarly revealed a large negative volume change, a small enthalpy change, and thus a significant positive entropy change on electron transfer. It is of interest to explore these issues in PS II using the same technique. In this work PTRPA was used to obtain the thermodynamic parameters of flash-induced electron-transfer reaction of the purified PS II core complexes from cyanobacterium *Synechocystis* sp. PCC 6803.

MATERIALS AND METHODS

Preparation of the Purified PS II Core Complexes. Purified oxygen-evolving PS II core complexes were prepared from the WT cyanobacterium *Synechocystis* 6803 as previously described (*11*, *12*). The Mn cluster was removed by treating the core complexes for 30 min at ~300 μg/mL with 5 mM NH_2OH plus 1 mM EDTA in buffer II (50 mM Mes, pH 6.0, 25% glycerol, 5 mM $CaCl_2$, 5 mM $MgCl_2$, and 0.03% DM) plus 30 mM $MgSO_4$. The cores were then passed though an Econo-Pak 10 DG desalting column equilibrated with buffer II only. The core complexes were then concentrated to ~200 μg of Chl/mL by spinning overnight in Centricon 100s (Millipore) according to the manufacturer's direction. All treatments were at 4 °C. The core complexes were stored at −80 °C until use. The glycerol was removed for PA measurements by centrifuging using Centriprep YM-50 (Millipore) and placed in the 10 mM Mes, Hepes, or Ches buffer and 0.03% DM. The chlorophyll to Q_A ratio was determined by the method described in ref *11* and showed that the purified PS II core complexes contain 40 Chl per photoreducible Q_A. These preparations were frozen and stored in liquid nitrogen prior to the PA measurements.

Photoacoustic Measurements. The procedure is similar to the methodology described elsewhere (*9*, *10*). Laser pulses of 5 ns at 625 and 674 nm were used to excite the PS II core complexes. The OD values of the PS II core complexes were adjusted to ~0.2 per mm at the excitation wavelengths for PA measurements. Global convolution analysis of PA data was performed according to the previous paper (*10*).

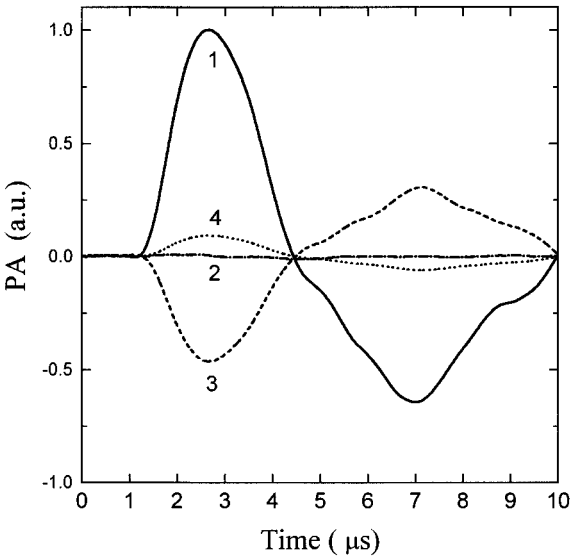

FIGURE 1: PA signal of the Mn-depleted PS II core complex and carbon ink reference: 10 mM Mes, pH 6.0, 0.03% DM, OD_{674} = 0.12/mm (~16 μg of Chl/mL), pulse energy 14 μJ cm^{-2} at 674 nm. Curve 1, carbon ink, 25 °C; curve 2, carbon ink, 3.7 °C; curve 3, PS II core complexes, 20 μM benzidine, 0.1 mM FeCy, 2 mM $CaCl_2$, 3.7 °C; curve 4, PS II core complexes with the same additions at 25 °C.

RESULTS

Photoacoustic Signals of PS II Core Complexes. The typical PA signals of isolated PS II core complexes are shown in Figure 1. In our experiments with PTRPA, we used flashes at 674 nm for excitation of the PS II core complexes. Curve 1 and curve 2 in Figure 1 are the PA signal of the thermal reference, carbon ink, at room temperature and at the temperature of maximum solution density, ~4 °C, respectively. As expected, the thermal PA signal was zero at ~4 °C. The photochemical reaction of PS II core complexes produces PA signals from two sources. The first is the thermal signal, which is heat released by the system in the measured time window. The other is the volume change of the reaction center itself following the photochemical reaction. At the temperature of maximum density of water, ~4 °C, the thermal signal disappears, leaving only the volume change of the reaction centers. The PA signal of Mn-depleted PS II core complexes of *Synechocystis* 6803 shows a volume contraction at ~4 °C (curve 3) but an expansion at 25 °C (curve 4). This observation is different from those of PS I trimer complexes from *Synechocystis* 6803 (*10*) and bacterial reaction centers from *Rb. sphaeroides* (*9*), which show negative signals even at room temperature. This implies that the enthalpy change of electron transfer in PS II is larger and/or the ΔV is smaller than that of PS I and bacterial centers.

As the averaging of several low-energy flashes is required, the recovery time of reaction centers must be measured in order to ensure that the centers have returned to their initial state before the next actinic pulse. Following the same protocol as in the preceding paper (*10*) we have determined the recovery time of the Mn-depleted PS II core complex of

Table 1: Photochemical and Thermodynamic Parameters of PS II Core Complexes from *Synechocystis* 6803

buffer[a]	λ_{ex}, nm	$\Phi\sigma$, Å^2	Φ,[b] %	ΔV_y,[c] Å^3	ΔV_s,[d] Å^3	TE_0, %	ΔH, eV	$T\Delta S$,[e] eV
pH 9.0, Ches	674	87 ± 9	83 ± 8	−3.4 ± 0.5[f]	−2.6 ± 0.5	37 ± 7[f]	−1.15 ± 0.13	−0.23 ± 0.13
pH 7.5, Hepes	674	104 ± 10	99 ± 10	−7.3 ± 2	−11.8 ± 2	43 ± 5	−1.04 ± 0.1	−0.27 ± 0.1
pH 6.0, Mes	625	32 ± 3	114 ± 15	−8.8 ± 1.0	−10.6 ± 2	52 ± 5	−0.9 ± 0.1	−0.1 ± 0.1

[a] Buffer concentrations are 10 mM with addition of 20 μM benzidine, 0.2 mM FeCy, 2 mM $CaCl_2$, and 0.03% DM. [b] The values of quantum yield Φ are obtained from the ratio of calculated optical cross sections of PS II, 105 and 28 Å^2 at 674 and 625 nm, respectively, to the effective optical cross sections $\Phi\sigma$. [c] The limiting value, in Å^3 per molecule, of the yield curve fit at low energies at 4 °C. [d] The maximum value, in Å^3 per molecule, at 4 °C when all reaction centers are excited. [e] ΔG is estimated to be −0.77 eV at pH 6−7.5 and −0.92 eV at pH 9.0 (from data in Tables 3 and 4). [f] With correction for the quantum yield of 83%.

Synechocystis 6803 in the presence of benzidine (20 μM) and FeCy (2 mM) at 4 °C. There are two components: a fast phase with a time constant of less than 0.1 s (11%) and a slow phase of 0.4 s (89%). Thus the recovery time of PS II is less than 1 s, and we used a pulse rate of 1 Hz at low excitation energy (<10% centers excited) and <0.5 Hz at near saturation energies to allow full recovery of the reaction centers.

We recorded the light saturation curve at ~4 °C and thus obtained the quantum yield of photochemistry of the samples using measured versus calculated optical cross sections (see ref *10* for details). Table 1 lists the quantum yield of photochemistry in PS II core complexes from *Synechocystis* 6803. The quantum yield of photochemisty in PS II was close to unity with two different preparations at pH 6 and 7.5 using two excitation wavelengths, 625 and 674 nm (Table 1). However, it decreased to 83 ± 8% at pH 9.0.

Volume Contraction. Light-induced charge separation produces a volume contraction in both PS I and PS II reaction centers. Comparing the amplitude of PA signals, we found that PS II showed a smaller PA signal than PS I.

We used two different methods to obtain the volume changes of the reaction centers near 4 °C: (1) volume yield method and (2) saturation method (see preceding paper, ref *10*). In the first method, as shown in Figure 2, increasing the excitation energy of the flash reduced the yield of the negative volume change. This is caused by multiexcitation of the "filled" reaction center and waste of energy. Therefore, the true volume contraction of the reaction center is that at the lowest excitation energy. However, the low energy produced a PA/E signal with significant error. To improve the signal-to-noise ratio, we used the curve fitting method to obtain the limiting volume change of the samples (Figure 2; see ref *10* for details). The results are listed in Table 1. It was found that the volume contraction of PS II is about −8.8 ± 1.0 Å^3 at pH 6.0, −7.3 ± 2 Å^3 at pH 7.5, and −3.4 ± 0.5 Å^3 at pH 9.0.

The second method uses the maximum PA signal of the reaction center of PS II. Surprisingly, the PA signal of PS II core reaction center decreases when the pulse energy exceeds ~100 μJ/cm^2 at 674 nm and ~200 μJ/cm^2 at 625 nm (Figure 3). This phenomenon may result from excitation of the initially photogenerated charge-separated state producing a large positive volume change ΔV_m, presumably by charge neutralization. We fit the curves with nonlinear least squares to the equation $\Delta V = \Delta V_s(1 - e^{-\Phi\sigma E}) + \Delta V_m(1 - e^{-\Phi\sigma E})(1 - e^{-\Phi\sigma_m E})$, where E is the photon energy absorbed by the sample, Φ is the quantum yield of the photochemical reaction, ΔV is the observed volume change, ΔV_s is the maximum volume change of charge separation in PS II, ΔV_m is that of the secondary reaction, and $\Phi\sigma$ and σ_m are the optical cross sections of the centers for charge separation in initial and for charge neutralization in charge-transferred states, respectively. As shown in Table 1, ΔV_s of ~−11 Å^3 and ~−3 Å^3 were obtained at pH 6 and pH 9, respectively. These data are in line with that of the first method. Because of the many unknowns (four) in this equation, we fixed the values of $\Phi\sigma$ to those obtained by the first method and of ΔV_m as $-2\Delta V_s$. The σ_m was found to be ~7 Å^2, independent of wavelength at 674 and 625 nm. This indicates that the target is not all the antenna chlorophyll molecules. The candidate is one or a few molecules with broad absorption spectra (*13*). This reaction was completely reversible, since no change in the volume contraction was observed at low flash energies after saturation experiments at 4 °C.

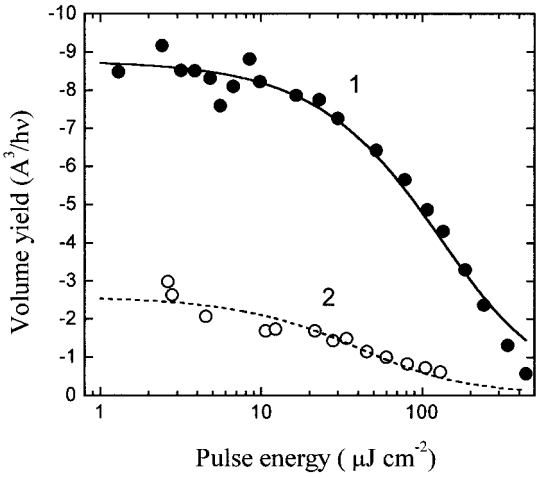

FIGURE 2: Volume yield of PS II core complexes versus light pulse energy at 3.7 °C: medium with 20 μM benzidine, 0.2 mM FeCy, 2 mM $CaCl_2$, 0.03% DM. The excitation area of the sample within the PA cell is about 1.43 cm^2. The fits are $\Delta V/E = \Delta V_y(1 - e^{-\Phi\sigma E})/(\sigma E)$. Curve 1 (closed circles): 10 mM Mes, pH 6.0, $OD_{625} = 0.106$/mm (~14 μg of Chl/mL), excitation at 625 nm; solid line is the fit with $\Phi\sigma = 32 \pm 4$ Å^2, $\Delta V_y = -8.7 \pm 2$ Å^3. Curve 2 (open circles): 10 mM Ches, pH 9.0, $OD_{674} = 0.151$/mm (~20 μg of Chl/mL), excitation at 674 nm; dashed line is the fit with $\Phi\sigma = 87 \pm 9$ Å^2, $\Delta V_y = -2.6 \pm 0.5$ Å^3.

Thermal Efficiency and Enthalpy. The positive PA signal of PS II at room temperature implied a lower thermal efficiency or significant enthalpy change of electron transfer in PS II. Using the difference of slopes of d(PAk)/dα of the PS II core reaction center and of the ink reference, where κ and α are the compressibility and expansivity of water, respectively, thermal efficiencies per trap of PS II on the microsecond time scale were obtained (see ref *10* for theory). The thermal efficiency per trap was found to be 52 ± 5% at pH 6.0. It decreased at higher pH values, 43 ± 5% at pH

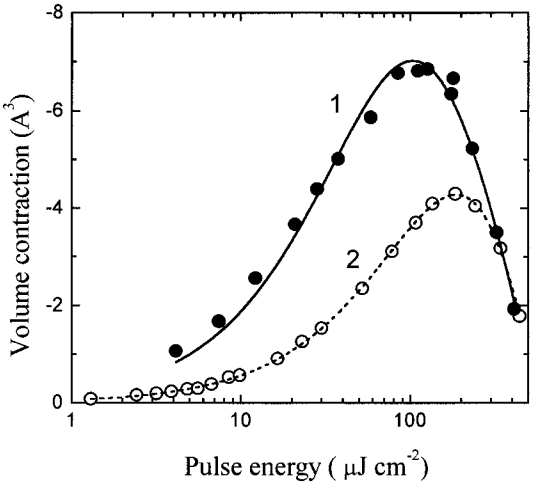

FIGURE 3: Saturation curves of PS II core complex volume change at 3.7 °C: medium with 20 μM benzidine, 0.2 mM FeCy, 2 mM $CaCl_2$, 0.03% DM. The excitation area of the sample within the PA cell is 1.43 cm^2. The fits are $\Delta V = \Delta V_s(1 - e^{-\Phi\sigma E}) - \Delta V_m(1 - e^{-\Phi\sigma E})(1 - e^{-\sigma_m E})$, assuming ΔV_m to be twice ΔV_s with opposite sign. Curve 1 (closed circles): 10 mM Hepes, pH 7.5, OD_{674} = 0.180/mm (~23 μg of Chl/mL), excitation at 674 nm; solid line is the fit with $\Delta V_s = -10.6 \pm 2$ Å^3, $\Phi\sigma = 105$ Å^2 (assumed, Table 1), $\sigma_m = 6.6 \pm 1$ Å^2. Curve 2 (open circles): 10 mM Mes, pH 6.0, OD_{625} = 0.106/mm (~14 μg of Chl/mL), excitation at 625 nm, dashed line is the fit with $\Delta V_s = -11.8 \pm 2$ Å^3, $\Phi\sigma = 32$ Å^2 (assumed, Table 1), $\sigma_m = 6.8 \pm 1$ Å^2.

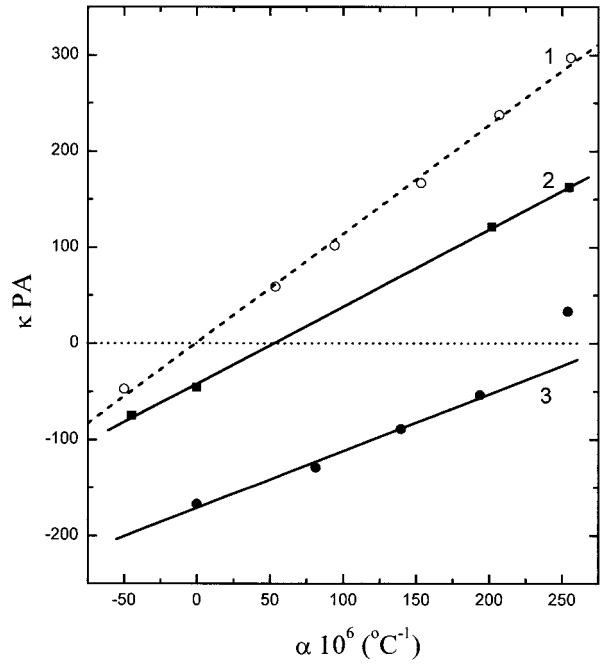

FIGURE 4: The product of the photoacoustic signal and water compressibility (κ) versus water thermal expansivity (α) for carbon ink reference and PS II core complexes: medium with 20 μM benzidine, 0.2 mM FeCy, 2 mM $CaCl_2$, 0.03% DM; OD_{674} = 0.12/mm (~16 μg of Chl/mL), excitation at 674 nm, pulse energy 6 μJ cm^{-2}. Curve 1 (open circles): carbon ink reference. Curve 2 (closed squares): 10 mM Ches, pH 9.0, solid line is the fit with TE_0 = 29%, $\Delta V = -2.6$ Å^3. Curve 3 (closed circles): 10 mM Mes, pH 6.0, solid line is the fit with TE_0 = 48%, $\Delta V = -10.3$ Å^3.

7.5 and 30 ± 7% at pH 9.0 (Table 1 and Figure 4). Since the quantum yield at pH 9.0 was 83% (Table 1), this increases the true thermal efficiency to 37%. These values are in line with the energy storage of ~40% in a similar PS II core preparation from *Chlamydomonas reinhardtii* reported by Delosme et al. (*14*). However, they are smaller than the value for PS II membranes from spinach (~60%) measured by the same authors (*14*). This discrepancy could be attributed to a contamination of PS I in the BBY preparation.

Table 2: Comparison of Analytical Results of Global Convolution and Peak-to-Peak PA Data for the PS II Core Complex[a]

method	ΔV_y, Å^3	TE_0, %	ΔH, eV	$T\Delta S$, eV
global analysis	−7.0 ± 2	45 ± 8	−1.0 ± 0.15	−0.23 ± 0.15
peak-to-peak analysis	−7.3 ± 1.5	43 ± 5	−1.04 ± 0.1	−0.27 ± 0.1

[a] pH 7.5, 10 mM Hepes; the excitation wavelength is 674 nm.

Taking the trap energy of the PS II reaction center, E_{trap} = 1.82 eV, the enthalpy of reaction in PS II in the time window of 0.1−10 μs is determined to be −0.9 ± 0.1 eV at pH 6.0, −1.0 ± 0.1 eV at pH 7.5, and −1.15 ± 0.2 eV at pH 9.0 (Table 1).

Global Analysis of Volume and Enthalpy Changes. The above thermodynamic data analysis was based on the peak-to-peak PA signals. Using a global convolution analysis of PA data under given conditions at all of the different temperatures and pH 7.5 between 4 and 25 °C, we obtained a thermal efficiency of 45 ± 8%, volume contraction of −7.0 ± 2 Å^3, and enthalpy of −1.0 ± 0.1 eV. These data agree with the peak-to-peak analysis (Table 2).

Kinetic Analysis by Convolution of PA Signals. The advantage of PTRPA is that data analysis by convolution can be used to obtain the time-resolved PA components (*15*, *58*). The acoustic pressure signal is caused by the rate of heat production. Thus the amplitude of the PA measurement is weighted by the rate constant of the heat producing step (*8*). The time window in the present study was 0.1−10 μs.

The $Y_Z \rightarrow P_{680}$ electron/proton transfer is dependent on pH (*17*−*18*, *28*, *44*, *45*). At pH ~6 this reaction occurs at room temperature in >10 μs and at pH ~9 in <1 μs. Using our convolution method we would expect to resolve the fast components at high pH unless they occur in <100 ns.

The fits of the entire time course of the PS II signal via convolution at pH 6.0 indicated that there were two negative components: a fast component of rise time <100 ns with ~90% amplitude and a 1−5 μs component with ~10% amplitude at 4 °C. The deconvolution showed no indications of a positive component (±20%) in our time window. In the case of pH 9.0 the convolution of PA data also resolved no positive PA component, which would be expected if cancellation of charge via Y_Z^- oxidation by P_{680}^+ occurred. Our results suffered from the small volume contraction observed and the limited signal-to-noise ratio, especially at pH 9.0.

DISCUSSION

Volume Contraction and Electrostriction. Charge separation in reaction centers induces a volume contraction via electrostriction that is revealed by pulsed photoacoustics. The reaction centers of *Rb. sphaeroides* undergo a −28 Å^3 per molecule volume contraction on excitation (*9*), and PS I trimer reaction centers contract by −26 Å^3 (*10*). What about the oxygenic photosynthetic reaction center of PS II?

Since the structure and organization of PS II is proposed to be similar to that of bacterial reaction centers (*20*, *21*),

the volume change of photoinduced charge separation of PS II is expected to be about the same. However, the observed volume contraction of PS II at pH 6.0 was only one-third this value and even smaller at higher pH (Table 1). This is not an artifact of the PA measurements or the low photochemical activity of our PS II samples as discussed below.

The quantum yield of PS II reaction centers is a very fundamental parameter, but there are no good data available in the literature. This parameter is often assumed to be unity. Using pulsed photoacoustics we were able to obtain these crucial data. As shown in Table 1, the quantum yield of Mn-depleted PS II core reaction centers from *Synechocystis* 6803 at pH 6 was determined to be 114 ± 15% from its effective optical cross section assuming the Chl/RC ratio of 40. Additional support is provided by the similar maximal volume change using both the yield and the saturation methods (Table 1). This finding indicates the quantum yield is close to unity since the yield method depends on the quantum yield and the saturation method does not. Thus the smaller volume contraction of PS II is not caused by a low yield. However, the quantum yield is lower (83%) at pH 9 (Table 1).

Arata and Parson (*59*) have proposed that the light-induced volume change of reaction centers is attributable to electrostriction, which has been described thermodynamically by Drude and Nernst (*22*). According to thermodynamics and electrostatics, the volume contraction is described by the extended Drude−Nernst equation for two ions of opposite charge:

$$\Delta V_{el} = \frac{\partial \Delta G_{el}}{\partial P} = \left(\frac{z^2 e^2 \kappa}{2\epsilon}\right)\left(\frac{\partial \ln \epsilon}{\partial \ln V}\right)\left[\frac{1}{r_+} + \frac{1}{r_-} - \frac{2}{r_\pm}\right] \quad (1)$$

where ΔV_{el} is electrostriction, ΔG_{el} is the Born charging energy, P is pressure, z is the charge on the spherical ions, κ is compressibility of the protein, V is its molar volume, ϵ is its dielectric coefficient, r_+ and r_- are the radii of the donor and acceptor (assumed previously neutral), and $r_\pm$ is the distance between the two ions.

Effect of Size of Ions on ΔV. The size of P_{700} in the PS I reaction center from *Synechocystis* 6803 is expected to be the same (or somewhat smaller because of less overlap and thus charge delocalization) as that of P_{870} of the bacterial reaction center of *Rb. sphaeroides*. But the radii of F_x, F_A, or F_B iron−sulfur centers (∼5.2 Å, an estimation in this paper, and 4.9 Å in ref *23*) are larger than that of Q_A (radius of ∼2.5 Å) in the reaction center of *Rb. sphaeroides*. It is thought that the core charge changes from +3 to +2 but is surrounded by four negative cysteinates bounded to the irons. From the viewpoint of electrostatics it is the total charge change −1 to −2 and the total volume of the charge delocalization over the Fe_4S_4(cysteinate)$_4$ complex that counts. Our estimate of this radius is 8 Å, and this leads to a predicted ΔV of ∼−23 Å^3. Together with the −8 Å^3 of the P_{700}^+ the total, −31 Å^3 is reasonably close to the observed −26 Å^3 (*10*). Also, the distance between P_{700} and F_A or F_B is about 42 or 54 Å (*24*, *25*), respectively, considerably larger than that between P_{870} and Q_A in reaction centers of *Rb. sphaeroides*, about 28 Å (*26*, *27*). Taking this change into account, the calculated volume contraction is −30 Å^3 for PS I. However, in the case of PS II, the observed volume contraction is unexpectedly small, ∼−9 Å^3 at pH 6.0 and ∼−3 Å^3 at pH 9.0. We use the Drude−Nernst equation to discuss the possible charge-transfer reactions.

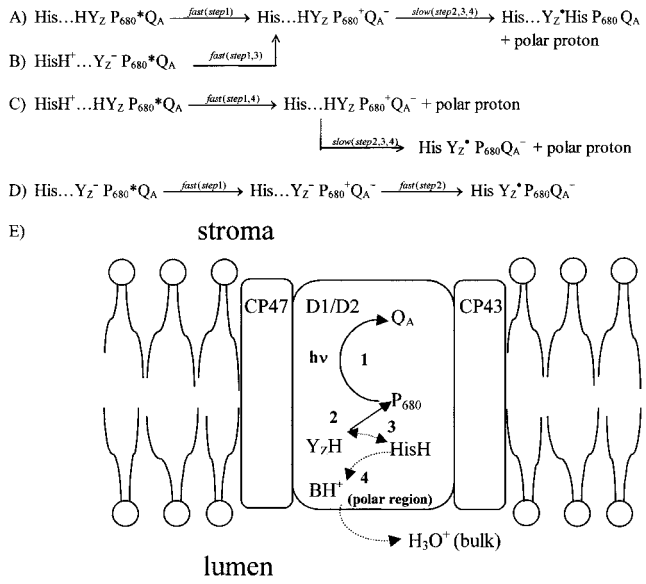

FIGURE 5: (A−D) Possible electron- and proton-transfer reactions in Mn-depleted PS II core complexes. (E) The solid line stands for the direction of electron transfer and the dashed line for proton transfer. D1/D2 are the reaction center core subunits. CP47 and CP43 are the peripheral light harvesting proteins. Upon the photoinduced charge separation (1), at pH 6 the electric field of the cation induces a fast proton transfer from protonated His near Y_Z (3), possibly D1-His-190. The proton is most likely released to the polar region (4) and then to the aqueous solution. At pH 9, proton transfer from Y_ZH to neutral histidine is induced (3), followed by electron (2) and proton transfer (4). The electron transfer from Y_Z^- to P_{680}^+ cancels the charges, induces a volume expansion, and thus gives a small volume change in the overall reaction. For details see text.

The pK_a for Y_Z has been estimated to be ∼7−8 (*17*, *28*) but see Hays et al. (*45*) for a contrary opinion, pK_a = ∼10. The electron donor to P_{680}^+, redox-active tyrosine Y_Z, would thus be deprotonated at pH 9.0 before it is oxidized by P_{680}^+ (Figure 5D). Therefore, at the time of light-induced charge separation, the electric field of the positive P_{680}^+ would be partly canceled by the negative charge of Y_Z^- at a distance of 12 Å (*2*). This would reduce the volume contraction around P_{680}^+ and can be calculated by an extension of eq 1 for three ions, using pairwise interactions, i.e., three ion−ion terms with appropriate signs. The calculation results in a volume contraction of −22 Å^3, ∼7 times that observed. By adding more negative charge near P_{680}, one could further decrease the electrostriction. However, all of this negative charge would decrease the redox potential of P_{680}, which is necessarily much higher than chlorophyll in solution and thus is unlikely to be present. If the transfer of charge from Y_Z^- to P_{680}^+ occurs in <100 ns, the electrostriction of both ions will vanish. It has been demonstrated that the oxidized $Y_Z^\bullet$ is a neutral radical (*17*, *29*; for a review see ref *6*). The resulting volume change for this reaction step, $Y_Z^- P_{680}^+ Q_A^- \rightarrow Y_Z^\bullet P_{680} Q_A^-$, is estimated to be +29 Å^3, taking a radius of 2.2 Å for Y_Z and distance 12 Å between Y_Z and P_{680} (*2*, *30*−*34*). It has been reported that the distance between Y_Z and Q_A is 32−35 Å (*35*−*38*). Using these values, the total volume change forming $Y_Z^\bullet$ and Q_A^- from Y_Z^- P_{680}*Q_A is then estimated to be +3 Å^3. The difference between this value and the observed −3 Å^3 is close to the error and could

be caused by some redox equilibration of Y_Z and P_{680}^+ or an ensuing change in protein conformation. Another possibility is that Y_Z may be incompletely deprotonated. It is estimated that ~60% of Y_Z may be deprotonated by the comparison of difference spectra (pH 6.0 minus pH 9.0) of oxidized-minus-reduced Y_Z with that (pH 7.4 minus pH 12) of tyrosine in water (*17*). The estimated ΔV is then -2 Å^3, using ΔV observed at pH 6 as the protonated ΔV (see below).

Optical measurements indicate that the charge transfer of P_{680}^+ to tyrosine Y_Z at acidic pH at room temperature in the absence of Mn occurs on the ≥ 10 μs time scale (*39*−*41*). All measurements of P_{680}^+ reduction and of Y_Z oxidation agree on a wide distribution of reaction times in the 10^{-8}−10^{-5} s range (*42*−*47*). The particular time constant and its contribution in amplitude vary widely depending on the presence or absence of the Mn cluster and in the case of the latter on the pH. The particular preparations used here have "most" of the P_{680}−Y_Z reaction occurring in >10 μs at pH 6 and ≤ 1 μs at pH 9 when measured by absorption changes at room temperature in the UV and visible region. A possible complication in the optical measurements is the use of high-intensity, saturating flashes. As shown clearly in our flash saturation curve (Figure 3), there is a decrease in $|\Delta V|$ at high flash energies. Our analysis shows that a secondary reaction causes a large, reversible, positive volume change indicating charge neutralization. If this reaction is a proton movement, it could be invisible optically. No such positive volume change is seen in PS I and bacterial reaction centers (*9*, *10*).

If only $P_{680}^+Q_A^-$ formation were observed at more acidic pH, a volume change of -28 Å^3 is expected, not the observed -3 to -9 Å^3. A possibility, much discussed in the literature (*17*, *19*, *28*, *44*, *45*), is that a base, histidine, is hydrogen bonded to Y_ZH (Figure 5A). The reaction $His\cdots HY_ZP_{680}{}^*Q_A \rightarrow His\cdots HY_ZP_{680}{}^+Q_A{}^-$ would produce a ΔV of -28 Å^3. If the field of the P_{680}^+ cation forced proton transfer from the tyrosine to the histidine, rapid electron transfer would occur: $His...HY_ZP_{680}{}^*Q_A \rightarrow [HisH^+\cdots Y_Z{}^-P_{680}{}^+Q_A{}^-] \rightarrow HisH^+\cdots Y_Z{}^\bullet P_{680}Q_A{}^-$. However, the estimated electrostriction would be -65 Å^3. Thus the charge of any proton involved must move to a more polar region in <100 ns. The overall reaction is $His\cdots HY_ZP_{680}{}^*Q_A \rightarrow His\cdots Y_Z{}^\bullet P_{680}Q_A{}^-$ + polar proton with estimated ΔV of ~ -25 Å^3. If proton transfer occurred in the complex, i.e., $HisH^+\cdots Y_Z{}^-P_{680}{}^*Q_A \rightarrow His\cdots Y_Z{}^\bullet P_{680}Q_A{}^-$ + polar proton, then the calculated electrostriction would be $+28$ Å^3 because of the small size of the histidine cation and loss of its electrostriction. Thus if some 40% of the tyrosine−histidine were in the ionized form, a ΔV of -6 Å^3 is predicted, as is observed. The solvent accessibility of Y_Z and Y_D by deuterium isotope effect on Y_Z oxidation and ESEEM technique demonstrated that the environment of Y_Z is more polar than that of Y_D (*17*, *57*). Kinetic measurements using site-directed mutants also showed that Y_Z is located in a significant polar region in contrast to Y_D (*44*). Thus the ionization of tyrosine by histidine is quite possible.

At pH 6.0, the histidine is expected to be protonated. On photoformation of the P_{680}^+ cation, its electric field will decrease the pK_a of the histidine, causing movement of the proton to the polar region (Figure 5B). The reaction is $HisH^+\cdots Y_ZHP_{680}{}^*Q_A \rightarrow His\cdots Y_ZHP_{680}{}^+Q_A{}^-$ + polar proton. The volume change calculated is $+6$ Å^3. An admixture of some nonprotonated histidine can account for the difference from observation.

Effect of Compressibility and Dielectric Coefficient on ΔV. What about the other parameters in the Drude−Nernst equation that we have assumed constant? The negative term $\partial \ln \epsilon / \partial \ln V$ is the change in relative ϵ with relative volume or reciprocal density. This is the least known term for proteins, but changes little even over a wide range of substances (*48*) and is why we write the equation in this form. The compressibility κ of proteins, when corrected for changes in hydration, is fairly constant (*49*, *50*) since they are usually close-packed. The dielectric coefficient, ϵ, of proteins is still a subject of some controversy, and the measurement of electrostriction may be a good way to obtain this important parameter (*16*). Accommodation of our observed ΔV in PS I would require only an increase of the effective dielectric coefficient from ~4 to ~5. However, accommodation of our data on PS II would require a tripling of the effective dielectric coefficient in PS II relative to bacterial reaction centers. An even greater increase is required at alkaline pH. This seems extravagant given that the proteins and their structure are quite similar.

An estimate of the effect of a higher dielectric (water $\epsilon = 80$) adjacent to the protein (effective $\epsilon = 4$−6, via electrostriction; Mauzerall, to be published) can be made by the method of images (*51*). Even if the polar interface is situated at the radius of the ion, the electrostriction would only be reduced by a factor of 2. Movement of the polar interface by another ion radius, i.e., having the ion $^1/_2$ in the polar region would however cause reduction by a factor of 8. Thus bulk water would have to be less than 7 Å from the center of P_{680}^+, and its contribution is only -8 Å^3 out of the -28 Å^3 expected. The water would also have to be less than 2 Å from Q_A^- to reduce its contribution to less than one-half, and that is not likely. Note that the distance of any of these ions to the water interface in the RC, radius of ~20 Å, is far less than the Coulomb radius (the distance where univalent ions interact with energy of *kT*), 270 Å in a protein of $\epsilon = 2$. The effective ϵ, 4−6, thus includes considerable effect of the nearby water as expected. As noted above and pointed out by Gilson et al. (*51*), the effective ϵ depends on the distance from the polar interface.

We conclude that our data are best accommodated by a mixture of neutral and anionic tyrosine and neutral and cationic histidine with ratios dependent on pH. A mixture of neutral (Figure 5A) and ionic forms (Figure 5B) would result in a small volume change. As the pH becomes more acidic, the histidine is protonated and the photoformed cation field forces the proton out (Figure 5C), with a volume change of $+6$ Å^3. The proton is most likely released to the polar region (step 4) and then to aqueous solution on a slower time scale. The steps are shown in Figure 5E. It was reported that the half-time of proton transfer to aqueous solution is ~40 μs in the Mn-depleted PS II reaction centers (*28*). If the base in the polar region is a carboxylate anion, e.g., glutamate, then a further contribution of "electroexpansion" will occur as charge is neutralized. As the pH becomes more alkaline, the tyrosine ionizes and the total charge transfer to Y_Z (Figure 5D) produces a volume change of $+3$ Å^3. A mixture of these forms will explain our observation as outlined above. Note that such a mixture guarantees several time constants for the oxidation of tyrosine Y_Z.

Table 3: Redox Potentials of Cofactors in the PS II Reaction Center

cofactor	E_m, V	reference
P_{680}^+/P_{680}	$+1.13 \sim 1.23$	*6* (theoretical limit)
P_{680}^+/P_{680}	$+1.12 \pm 0.05$	*52* (exptl estimation)
Q_A/Q_A^-	-0.08	*53* (O_2-evolving PS II)
Q_A/Q_A^-	$+0.065$	*53* (apo-PS II)
$Y_Z^{\bullet}/Y_Z^-$	$+0.97 \pm 0.02$	*54*

Table 4: Free Energy of Electron Transfer in the PS II Reaction Center

electron-transfer reaction	ΔG, eV	reference
$Y_Z^-P_{680}^+ \rightarrow Y_Z^{\bullet}P_{680}$	-0.075	*41* (pH 5.0, apo-PS II)
$Y_Z^- P_{680}^+ \rightarrow Y_Z^{\bullet}P_{680}$	-0.12	*55* (pH 6.0, apo-PS II)
$Y_Z^-P_{680}{}^*Q_A \rightarrow Y_Z^{\bullet}P_{680}Q_A^-$	-0.92	estimated from Table 3 for apo-PS II
$P_{680}{}^*Q_A \rightarrow P_{680}^+Q_A^-$	-0.77	estimated from Table 3 for apo-PS II

Enthalpy. The pulsed, time-resolved photoacoustic methodology that we have developed is suitable for investigation of the thermodynamics of photosynthetic systems on a nanosecond to microsecond time scale. By use of this method we have successfully measured the enthalpy of charge separation in reaction centers of *Rb. sphaeroides* (*9*) and PS I reaction centers of *Synechocystis* 6803 (*10*). Here the enthalpy of electron transfer in PS II was obtained at different pH values. The enthalpy of reaction at pH 6.0 is -0.9 ± 0.1 eV, -1.0 ± 0.1 eV at pH 7.5, and -1.15 ± 0.2 eV at pH 9.0 (Table 1). Comparing the enthalpy of electron transfer in the bacterial reaction center of *Rb. sphaeroides* (-0.44 eV) and the PS I reaction center (-0.39 eV), the large enthalpy of PS II reaction centers is surprising.

The electron-transfer reaction in PS II core complexes, involving Y_Z oxidation in this study on the 1 μs time scale, is coupled with proton transfer. In the case of bacterial and PS I reaction centers, it is a pure electron-transfer process on the same time scale. The large enthalpy change in PS II may be produced by the rapid proton-transfer step associated with electron transfer.

Entropy. The entropy of electron-transfer reactions is often assumed to be zero. However, recent photoacoustic studies have shown that such an assumption may not be true (*8*−*10*). Using the triplet state of zinc uroporphyrin in aqueous solution as electron donor and naphthoquinone-2-sulfonate as electron acceptor, it has been demonstrated that the entropy of this electron-transfer reaction is quite large and negative, -0.6 eV, as expected for a liquid (*8*). The recent PA data of bacterial reaction centers of *Rb. sphaeroides* (*9*) and PS I (*10*) revealed unexpected positive entropies, which have been attributed to bound counterion release.

The electron-transfer rate in Mn-depleted PS II core complexes depends on the pH of the solution. At high pH ($\sim$9.0) it is proposed that the electron can transfer from Y_Z to P_{680}^+ in <1 μs (*17*, *44*, *45*) at room temperature. If so, we may estimate the apparent entropy of the reaction for formation of $Y_Z^{\bullet}Q_A^-$ from excited P_{680}*. Note that we refer to an apparent entropy since the free energy may be different in an unrelaxed state of the protein (*9*). The $T\Delta S$ is -0.23 ± 0.13 eV, assuming the free energy is -0.92 eV (Tables 3 and 4). If at pH 6 the reaction only proceeds to $P_{680}^+Q_A^-$, with free energy of -0.77 eV, the $T\Delta S$ is -0.1 ± 0.1 eV. If this reaction occurs with a deprotonation of histidine (see above on ΔV) with pK_a = 6.9−7.5 (before charge separation), then ΔG will increase by 0.1 eV (pK_a < 6 after charge separation) and $T\Delta S$ will decrease to -0.2 eV.

Thus we conclude that the entropy of electron transfer in PS II core reaction center is small but negative no matter what the pH of the solution, in contrast with those of PS I and bacterial centers. Since the unexpected positive entropy of the bacterial and PS I centers was assigned to the liberation of counterions by charge neutralization on charge formation, this process does not occur in PS II centers since there is no charge formation on the microsecond time scale.

Comparison of the Thermodynamics of Electron Transfer in Bacterial, PS I, and PS II Centers. The volume changes (-28 Å^3) for the formation of $P_{870}^+Q_A^-$ in the bacterial reaction centers and that of PS I (-26 Å^3) forming $P_{700}^+F_A/F_B^-$ are quite similar (*9*, *10*). In the present paper a smaller volume contraction, about -9 Å^3 for the formation of $Y_ZP_{680}^+Q_A^-$ and about -3 Å^3 for $Y_Z^{\bullet}Q_A^-$, in PS II is measured. The former data can be explained by electrostriction, but assuming similar dielectric and thermoelastic properties, the data on PS II require that if the donor is P_{680}, it be linked to rapid proton expulsion, and if tyrosine is the donor, it must be partly in the anionic form. Proton transfer to polar environment must occur in <100 ns.

The enthalpies of electron transfer in bacterial and PS I reaction centers were found to be -0.44 and -0.35 eV, respectively (9, *10*). The similar differences in redox potentials of the donor and acceptor produce similar entropies of reaction. However, our PA data indicate that the enthalpy change of photochemistry on the 1 μs time scale in PS II is larger (-1 eV) than that of PS I and bacterial reaction centers (-0.4 eV). The entropy of electron transfer in PS II is negative, which is normal for charge formation in solution (*8*). The electron-transfer reaction in PS II is associated with proton transfer, which is favored by a more polar environment in the complex. Overall, our thermodynamic data of bacterial, PS I, and PS II reaction centers show that the entropy of electron transfer is complex and depends on the microenvironment of the protein and may involve coupling with proton transfer in PS II. This complexity of electron- and electron/proton-transfer reactions requires detailed and systematic studies using pulsed photoacoustics in order to understand the mechanism of electron transfer in photosynthetic systems.

Recently, we have obtained in vivo PA data of PS I and PS II in *Synechocystis* using selective excitation wavelengths. This has revealed volume contractions of about -27 Å^3 (PS I) and -2 Å^3 (PS II) and enthalpy values of -0.4 eV (PS I) and -1 eV (PS II) (*56*). These findings provide strong supporting evidence of our in vitro studies using purified PS I and PS II complexes from the same cyanobacterium.

If our hypothesis of proton transfer in PS II is correct, it must occur in <100 ns, too fast to be time-resolved using microsecond pulsed photoacoustics. We have developed a fast pulsed, time-resolved photoacoustics setup with time resolution of <10 ns. Experiments with this cell may allow one to time-resolve the components of the $Y_Z^- \rightarrow P_{680}^+$ reaction which we predict to have large and opposite volume changes. Another test would be Y_Z -less mutant [e.g., D1-Tyr161Phe (*55*)] PS II core complexes, which is expected to form $P_{680}^+Q_A^-$ upon photoinduced charge separation on

a microsecond time scale. This preparation would enable one to measure the volume contraction and enthalpy producing the $P_{680}^{+}Q_A^{-}$ from excited P_{680}* without interruption of the electron/proton-transfer step from Y_Z.

CONCLUSION

We obtained thermodynamic data on primary photoreactions of PS II core reaction center complexes from the cyanobacterium *Synechocystis* sp. PCC 6803 using pulsed photoacoustics. Volume contraction was determined to be -8.8 ± 1.0 Å^3 at acidic pH (6.0) and -2.8 ± 0.5 Å^3 at alkaline pH (9.0) on the 1 μs time scale. On the basis of estimations of electrostriction using the Drude−Nernst equation and experimental ΔV values of PS II, we propose that (1) the pH dependence is caused by a mixture of protonated and nonprotonated states of Y_Z and (2) fast proton transfer is involved in these reactions. The enthalpy of the electron-transfer reaction in PS II on the 1 μs time scale is -0.9 ± 0.1 eV at pH 6.0 and -1.15 ± 0.13 eV at pH 9.0, respectively. These data allow one to calculate a negative apparent entropy change ($T\Delta S = -0.1 \pm 0.1$ eV at pH 6.0 and -0.23 ± 0.1 eV at pH 9.0) for electron transfer from P_{680} and Y_Z to Q_A in PS II. These values differ considerably from those of PS I and bacterial centers.

ACKNOWLEDGMENT

We are grateful to William Parson, Kai Sun, and Gregory Edens for insightful discussions. We thank Irene Zielinski-Large and Jamie Wang for excellent technical assistance.

REFERENCES

1. Ort, D., and Yocum, C. F., Eds. (1996) *Oxygenic Photosynthesis*: *The Light Reactions*, Kluwer Academic Publishers, Dordrecht, The Netherlands.
2. Zouni, A., Witt, H. T., Kern, J., Fromme, P., Krauss, N., Saenger, W., and Orth, P. (2001) *Nature 409*, 739−743.
3. Blankenship, R. E., Madigan, M. T., and Bauer, C. E., Eds. (1995) *Anoxygenic Photosynthetic Bacteria*, Kluwer Academic Publishers, Dordrecht, The Netherlands.
4. van Grondelle, R., Dekker, J. P., Gillbro, T., and Sundstrom, V. (1994) *Biochim. Biophys. Acta 1187*, 1−65.
5. Diner, B. A., and Babcock, G. T. (1996) in *Oxygenic Photosynthesis: The Light Reactions* (Ort, D., and Yocum, C. F., Eds.) pp 213−247, Kluwer Academic Publishers, Dordrecht, The Netherlands.
6. Tommos, C., and Babcock, G. T. (2000) *Biochim. Biophys. Acta 1458*, 199−219.
7. Mauzerall, D., Feitelson, J., and Prince, R. (1995) *J. Phys. Chem. 99*, 1090−1093.
8. Feitelson, J., and Mauzerall, D. (1996) *J. Phys. Chem. 100*, 7698−7703.
9. Edens, G. J., Gunner, M. R., Xu, Q., and Mauzerall, D. (2000) *J. Am. Chem. Soc. 122*, 1479−1485.
10. Hou, J.-M., Boichenko, V., Wang, Y.-C., Chitnis, P. R., and Mauzerall, D. (2001) *Biochemistry 40*, 7109−7116.
11. Rogner, M., Nixon, P., and Diner, B. (1990) *J. Biol. Chem. 265*, 6189−6196.
12. Tang, X.-S., and Diner, B. A. (1994) *Biochemistry 33*, 4594−4603.
13. Davis, M. S., Forman, A., and Fajer, J. (1979) *Proc. Natl. Acad. Sci. U.S.A. 76*, 4170−4174.
14. Delosme, R., Beal, D., and Joliot, P. (1994) *Biochim. Biophys. Acta 1185*, 56−64.
15. Zhang, D., and Mauzerall, D. (1996) *Biophys. J. 71*, 381−388.
16. Mauzerall, D., Gunner, M. R., and Zhang, J. W. (1995) *Biophys. J. 68*, 275−280.
17. Diner, B. A., Force, D. A., Randall, D. W., and Britt, R. D. (1998) *Biochemistry 37*, 17931−17943.
18. Conjeaud, H., and Mathis, P. (1980) *Biochim. Biophys. Acta 590*, 353−359.
19. Debus, R. J., Campbell, K. A., Peloquin, J. M., Pham, D. P., and Britt, R. D. (2000) *Biochemistry 39*, 470−478.
20. Trebst, A. (1986) *Z. Naturforsch. 41c*, 240−245.
21. Michel, H., and Deisenhofer, J. (1988) *Biochemistry 27*, 1−7.
22. Drude, P., and Nernst, W. (1894) *Z. Phys. Chem. 15*, 79−85.
23. Setif, P., and Brettel, K. (1993) *Biochemistry 32*, 7846−7854.
24. Schubert, W. D., Klukas, O., Krauss, N., Saenger, N., Fromme, P., and Witt, H. T. (1995) in *Photosynthesis: from Light to Biosphere* (Mathis, P., Ed.) Vol. 2, pp 3−10, Kluwer Academic Publishers, Dordrecht, The Netherlands.
25. Krauss, N., Schubert, W. D., Klukas, O., Fromme, P., Witt, H. T., and Saenger, W. (1996) *Nat. Struct. Biol. 3*, 965−969.
26. Dzuba, S. A., Gast, P., and Hoff, A. J. (1995) *Chem. Phys. Lett. 236*, 595−602.
27. Yeates, T. O., Komiya, H., Rees, D. V., Allen, J. P., and Feher, G. (1987) *Proc. Natl. Acad. Sci. U.S.A. 84*, 6438−6442.
28. Ahlbrink, R., Haumann, M., Cherepanov, D., Bogershausen, O., Mulkidjanian, A. and Junge, W. (1998) *Biochemistry 37*, 1131−1142.
29. Berthomieu, C., Hienerwadel, R., Boussac, A., Breton, J., and Diner, B. A. (1998) *Biochemistry 37*, 10547−10554.
30. Xiong, J., Subramaniam, S., and Govindjee (1998) *Photosynth. Res. 56*, 229−254.
31. Mulkidjanian, A. Y., Cherepanov, D. A., Haumann, M., and Junge, W. (1996) *Biochemistry 35*, 3093−3107.
32. Hoganson, C. W., and Babcock, G. T. (1989) *Biochemistry 28*, 1448−1454.
33. Rutherford, A. W. (1986) *Biochem. Soc. Trans. 14*, 15−17.
34. Svensson, B., Etchebest, C., Tuffery, P., van Kan, P., Smith, J., and Styring, S. (1996) *Biochemistry 35*, 14486−14502.
35. Zech, S. G., Kurreck, J., Renger, G., Lubitz, W., and Bittl, R. (1999) *FEBS Lett. 442*, 79−82.
36. Zech, S. G., Kurreck, J., Eclert, J. K., Renger, G., Lubitz, W., and Bittl, R. (1997) *FEBS Lett. 414*, 454−456.
37. Jeschke, G., and Bittl, R. (1998) *Chem. Phys. Lett. 394*, 323−331.
38. Shigemori, K., Hara, H., Kawamori, A., and Akabori, K. (1998) *Biochim. Biophys. Acta 1363*, 187−198.
39. Reinman, S., and Mathis, P. (1981) *Biochim. Biophys. Acta 635*, 249−258.
40. Reinman, S., Mathis, P., Conjeaud, H., and Stewart, A. (1981) *Biochim. Biophys. Acta 635*, 429−433.
41. Buser, C. A., Thompson, L. K., Diner, B. A., and Brudvig, G. W. (1990) *Biochemistry 29*, 8977−8985.
42. Christen, G., and Renger, G. (1999) *Biochemistry 38*, 2068−2077.
43. Christen, G., Seeliger, A., and Renger, G. (1999) *Biochemistry 38*, 6082−6092.
44. Hays, A. A., Vassiliev, I. R., Golbeck, J. H., and Debus, R. J. (1998) *Biochemistry 37*, 11352−11365.
45. Hays, A. A., Vassiliev, I. R., Golbeck, J. H., and Debus, R. J. (1999) *Biochemistry 38*, 11851−11865.
46. Haumann, M., Mulkidjanian, A., and Junge, W. (1999) *Biochemistry 38*, 1258−1267.
47. Hundelt, M., Hays, A. A., Debus, R. J., and Junge, W. (1998) *Biochemistry 37*, 14450−14456.
48. Hamann, S. D. (1974) in *Modern Aspects of Electrochemistry* (Conway, B. E., and Bockris, J. O. M., Eds.) Vol. 9, pp 47−158, Plenum Press, New York.
49. Chalikian, T. V., Sarvazyan, A. P., and Breslauer, K. J. (1994) *Biophys. Chem. 51*, 89−109.
50. Chalikian, T. V., and Breslauer, K. J. (1998) *Curr. Opin. Struct. Biol. 8*, 657−664.
51. Gilson, M. K., Rasjom, A., Fine, R., and Honig, B. (1985) *J. Mol. Biol. 184*, 503−516.
52. Klimov, V. V., Allakhverdiev, S. I., Demeter, S., and Krasnovskii, A. A. (1979) *Dokl. Akad. Nauk SSSR 249*, 227−230.
53. Krieger, A., Rutherford, A. W., and Johnson, G. N. (1995) *Biochim. Biophys. Acta 1229*, 193−201.
54. Vass, I., and Styring, S. (1991) *Biochemistry 30*, 830−839.

55. Metz, J. G., Nixon, P. J., Rogner, M., Brudvig, G. W., and Diner, B. A. (1989) *Biochemistry 28*, 6960−6969.
56. Boichenko, V. A., Hou, J.-M., and Mauzerall, D. (2001) *Biochemistry 40*, 7126−7132.
57. Tommos, C., McCracken, J., Styring, S., and Babcock, G. T. (1998) *J. Am. Chem. Soc. 120*, 10441−10452.
58. Rudzki-Small, J., Libertini, L. J., and Small, E. W. (1992) *Biophys. Chem. 42*, 29−48.
59. Arata, H., and Parson, W. (1981) *Biochim. Biophys. Acta 636*, 70−81.

BI010373S